arXiv:1608.06456v1 [cond-mat.soft] 23 Aug 2016

Discontinous change from thermally- to geometrically- dominated effective interactions in colloidal solutions

Nicoletta Gnan, Francesco Sciortino and Emanuela Zaccarelli
CNR-ISC UOS Sapienza, Piazzale A. Moro 2, 00185 Roma, Italy and
Dipartimento di Fisica, "Sapienza" Universita' di Roma, Piazzale A. Moro 2, 00185 Roma, Italy

We report numerical results on the effective potential arising between two colloids immersed in a self-assembling cosolute which forms reversible clusters. The potential is evaluated at cosolute state points with different densities and temperatures but with the same connectivity properties. We find that the range of the resulting effective potential is controlled only by the cosolute thermal correlation length rather than by its connectivity length. We discuss the significant differences with previous results focused on cosolute forming irreversible clusters and we show that irreversible bond case represents a singular limit which cannot be accessed by continuously increasing the bond lifetime.

I. INTRODUCTION

The investigation of effective interactions in soft matter has a long history and provides the main theoretical framework to treat highly complex systems with many degrees of freedom experiencing several time and length scales[1]. Since the pioneering work of Asakura and Oosawa on depletion interactions, the addition of a non-interacting cosolute has become a fundamental tool to manipulate and control the phase behavior of colloidal suspensions[2–13]. More recently, it has become clear that also the cosolute properties can be exploited, not only to induce simple depletion effects, but also to give rise to new types of effective interactions among colloidal particles.

The prototype of this situation is that of colloidal particles interacting through the so-called "critical Casimir forces"[14], occurring whenever colloids are in solution with a solvent [15–18] or with a cosolute[19–21] close to a second-order critical point. Such forces are indeed arising because of the confinement of thermal critical fluctuations between the surfaces of the colloids; this generates a long-ranged effective potential which has, for fluids belonging to the Ising universality class, an exponential tail whose range is controlled by the correlation length of the critical fluid[14, 20, 22]. The experimental confirmation of critical Casimir forces[15, 23] has opened a new research avenue for generating colloidal aggregation [16, 19, 20, 24, 25] and stable colloidal phases [17, 26, 27] since the range of the potential can be reversely modified by simply tuning the temperature close to the critical point.

Casimir-like effects are very general, occurring whenever the fluctuations of an arbitrary order parameter are confined between two surfaces. Besides the famous quantum effects, classical analogues exploit fluctuation-induced phenomena and have been recently explored under thermal gradients[28], in active baths[29, 30], in granular materials[31], in driven diffusive systems [32] or in out-of-equilibrium conditions[33].

In a recent work [34] we have shown that it is also possible to exploit the analogy between a second order critical point and the percolation transition to induce a Casimir-like effective force among colloids. In particular, by performing numerical calculations of the effective potential between two hard sphere (HS) colloids immersed in a sol of clusters close to its gelation point, we have found that the confinement of the clusters-size fluctuations between the colloids surface gives rise to a long-range effective force, whose properties depend on the universal nature of percolation in analogy with the critical Casimir effect where the force is controlled by the universal properties of critical phenomena. In this context, we have also shown that the force can also be interpreted as a depletion force exerted by a highly polydisperse medium. Indeed the resulting effective potential between the two colloids can be described, for sufficiently low density, via a generalized Asakura-Oosawa model taking into account the polydispersity associated to the cluster size distribution of the sol. Interestingly, we found that the range of the effective potential is controlled by the connectivity length of the sol which reflects the clustering properties of the medium; this means that, independently on the density, whenever the cluster size distribution is the same, the effective potential close to percolation always displays the same range. These striking results occur when colloids are suspended in a so-called "chemical" sol, i.e. a cosolute in which the clusters have infinite lifetime and therefore can be treated as particles interacting via excluded volume among them and with the colloids in solution. Such situation is relevant for specific experimental conditions where such irreversible clusters can be achieved either by the use of chemical reactions in the sol or when the lifetime of the clusters is significantly longer than the experimental time scales (i.e. experiments that probe only a single sol microstate). However often clusters are reversible, breaking and reforming during the course of an experiment, and thus it is legitimate to ask how the results described above depend on the lifetime of the clusters in the sol.

To tackle this question, in this work we study the behavior of the effective potential between colloids immersed in a "physical" sol, where clusters are fully reversible, for a series of state points at different tempera-

tures and densities close to percolation, but having identical cluster size distribution. We show that such different state points do have different structural properties which are reflected in the effective potential arising when two colloids are put in the solution. Thus, we find that the range of the effective potential increases when the sol becomes more and more correlated, because it is controlled by the thermal correlation length (rather than by the connectivity length) of the sol. Comparing with the irreversible case, we thus find a drastic difference in the behavior of the effective potential. To rationalize this difference, we also study the effect of the bond lifetime by introducing an artificial barrier in the sol potential as previously used in [35–37], which does not alter the structural properties of the sol but only its dynamics. We find that, as long as the bond lifetime remains finite, albeit long, colloids will always experience the reversible effective potential, which remains always distinct physically and conceptually from the irreversible one.

II. MODEL AND METHODS

We first investigate the thermodynamic and geometric properties of the cosolute, that is modelled through a pairwise anisotropic Kern-Frenkel [38] three-patches (3P) potential. This amounts to consider particles as hard spheres of diameter σ with three attractive sites, located on the equator. The interaction $V_{\alpha\beta}^{SW}(|\vec{r}_{ij}|)$ between two sites α and β of two particles i and j at a center-to-center distance $\vec{r}_{ij}$ is a square-well of width $\delta = 0.119$ and depth $\varepsilon = 1$

$$V_{\alpha\beta}^{SW}(|\vec{r}_{ij}|) = \begin{cases} \infty & \text{if} \quad |\vec{r}_{ij}| < \sigma, \\ -\varepsilon & \text{if} \quad \sigma \leq |\vec{r}_{ij}| \leq \sigma(1+\delta), \\ 0 & \text{otherwise.} \end{cases} \tag{1}$$

modulated by an angular function G that depends on the orientation of the particles:

$$G(\hat{r}_{ij}, \hat{r}_{i\alpha}, \hat{r}_{j\beta}) = \begin{cases} 1 \text{ if } & \begin{cases} \hat{r}_{ij} \cdot \hat{r}_{i\alpha} > \cos(\theta_{max}), \\ -\hat{r}_{ij} \cdot \hat{r}_{j\beta} > \cos(\theta_{max}), \end{cases} \\ 0 & \text{otherwise.} \end{cases} \tag{2}$$

In the expression above $\cos(\theta_{max})$ accounts for the volume available for bonding and its value is set to $\cos(\theta_{max}) = 0.894717$. The total interaction potential reads as:

$$V_{ij,\alpha\beta} = V_{\alpha\beta}^{SW}(|\vec{r}_{ij}|) G(\hat{r}_{ij}, \hat{r}_{i\alpha}, \hat{r}_{j\beta}), \tag{3}$$

.

Here σ and ε are chosen as units of length and energy. We thus perform Monte Carlo (MC) simulations in the canonical ensemble of $N = 10836$ particles at several distinct temperatures and densities.

To evaluate the effective potential V_{eff} we perform Monte Carlo simulations of two large HS colloids (of diameter ten times larger than that of the cosolute particles) in solution with $3P$ particles for several state points. V_{eff} is evaluated by constraining the two colloids to move along the x-axis of a parallelepipedal box where the length of the x-edge $L_x = 70\sigma_s$ is twice and half the length of L_y and L_z. This guarantees that, for the simulated state points, the surface-to-surface distance between colloids is always larger than the distance at which V_{eff} goes to zero. In order to reduce the computational time, we use an umbrella sampling technique that allows us to run parallel simulations in which the two colloids sample only a limited range Δ_i of distances. In each simulation run, we evaluate the probability of finding the two colloids at a given distance $P(r, \Delta_i)$. Since different runs are allowed to have a small overlap in the probed Δ_i, we can obtain the total $P(r)$ by splicing together consecutive windows. Finally we extract the effective potential as $\beta V_{eff} = -ln(P(r))$, except for a constant that is set by imposing $V_{eff}(\infty) = 0$.

To modify the bond lifetime without altering the thermodynamics, we add an infinitesimally thin barrier to the edge of the square well potential among patches, following [36]. This is shown in Fig. 1

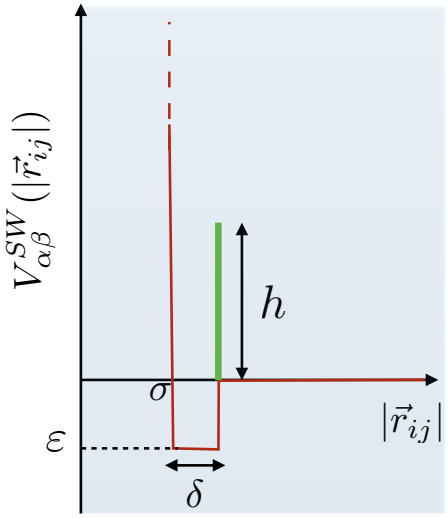

Figure 1. A sketch of the modified SW interaction between 3P particles where an infinitesimally-thin barrier (green thick line) of finite height h is also considered.

The barrier has a finite height h modulating the lifetime of the bonds among particles. We thus perform Monte Carlo simulations in the presence of the barrier by applying a modified Metropolis rule that account for the energy cost to overcome the barrier in forming /breaking bonds.[39]

To measure the bond lifetime, we compute that bond autocorrelation functions, defined as,

$$\phi_B(t) = \frac{\langle \sum_{i,j} n_{ij}(0) n_{ij}(t) \rangle}{N_b(0)} \tag{4}$$

where n_{ij} is 1 if particles i, j are bonded, zero otherwise and $N_b(t)$ is the total number of bonds in the system at

time t. Thus, the bond lifetime τ_B is defined as $\phi_B(\tau_B) = 1/e$.

III. RESULTS

A. Properties of the cosolute along constant bond probability loci (iso-p_b lines)

The $3P$ system belongs to the class of low-valence patchy models[40], thus displaying a gas-liquid critical point at low densities and the possibility to form equilibrium gels. The phase diagram of the 3P model is shown in Fig. **??** together with the simulated state points of this work. The gas-liquid coexistence line evaluated from Wertheim's theory [41–44] is reported together with the corresponding simulation results[45].

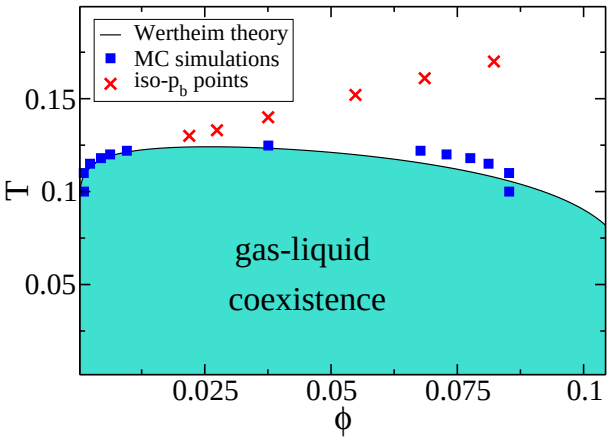

Figure 2. Gas-liquid coexistence line (blue squares) of the 3-patch particles model evaluated from Monte Carlo simulations[45]. The critical point is found at $(T = 0.125, \phi = 0.072)$, together with the corresponding theoretical calculations (black line) using Wertheim's theory. The figure also shows the simulated state points (red crosses) of constant bond probability p_b with $p_b \sim 0.565$ investigated in this work.

Since the connectivity properties of the sol (e.g. the probability of forming bonds) depend on temperature T and density ρ, it is possible to tune T and ρ in order to find state points of equal bond probability (p_b), drawing a line in the gas-liquid phase diagram which can be considered a precursor of the percolation line [46, 47]. Figure 3 shows p_b as a function of T for different densities. Solid lines are predictions from Wertheim's theory which well interpolate numerical results for a wide range of densities as shown also in [45]. For the model employed here, the bond probability is given by $-E/(fN)$ where E is the total potential energy, N is the total number of particles and f is the maximum number of bonds that a particle can form: for a $3P$ particle $f = 3$. Note that the percolation transition for this model has been estimated to take place at $p_c \simeq 0.618$ [34]. We thus select state points having a bond probability $p_b = 0.565 \pm 0.010$ at a relative distance to percolation $p_b/p_c = 0.92$, which are also reported in Fig. **??**. Along this line the distribution $n(s)$ of clusters of size s is found to be the same within numerical precision (inset of Fig. 3) in agreement with Flory-Stockmayer predictions[48], valid in the absence of bond loops, stating that the cluster size distribution only depends on p_b. This means that upon varying T and ϕ along the chosen iso-p_b line, particles aggregate into clusters of similar polydispersity with the same probability. Although the aggregation properties are similar, the structure of the sol is quite different along the iso-p_b line as shown by the radial distribution functions $g(r)$ and by the static structure factors $S(q)$ reported respectively in Fig. 4 and 5. The different structure of the sol reflects the progressive dilution of the clusters and the increased proximity to the gas-liquid spinodal at low ρ and T. Both effects contribute to the small wave vector increase of $S(q)$. Similarly the radial distribution functions $g(r)$ becomes progressively more structured on lowering the density, as shown in Fig. 4 (main panel and lower inset). Two features are interesting: the intense peak between σ and $\sigma(1+\delta)$ reflecting the presence of bonded pairs and the onset of a long range correlation, highlighted by the approach of the radial distribution function to one from above. These two features are indicated in more details in the two insets. In the upper inset of Fig. 4 all the peaks of $\rho g(r)$ superimpose to a good approximation, consistent with the iso-p_b constraint.

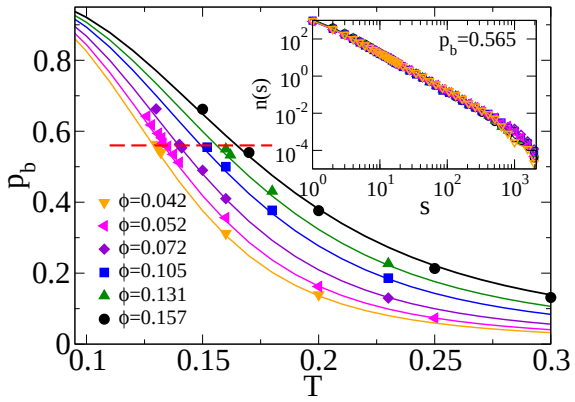

Figure 3. Bonding probability as a function of T for different densities. Symbols are results from MC simulations while solid lines are predictions from Wertheim's theory. The dashed lines selects state points with $p_b \simeq 0.565$. Inset: Cluster size distribution $n(s)$ for different densities along the $p_b \sim 0.565$ locus. $n(s)$ is the same within the numerical precision.

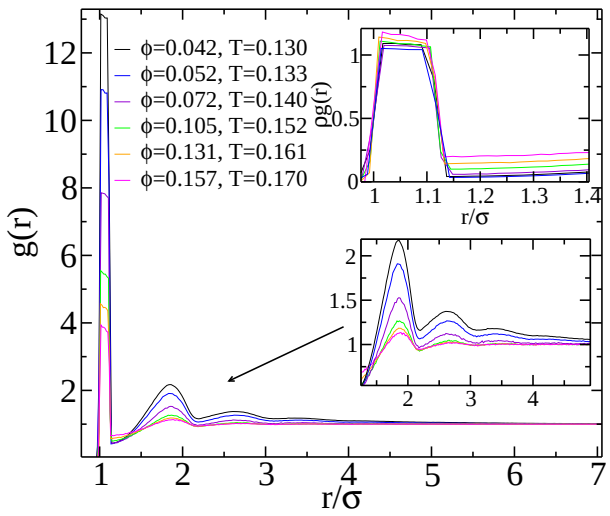

Figure 4. (a) Radial distribution functions $g(r)$ along the iso-p_b line. Insets: (b) $\rho g(r)$ to highlight the iso-p_b condition; (c) magnification at longer-r of the $g(r)$ along the iso-p_b line.

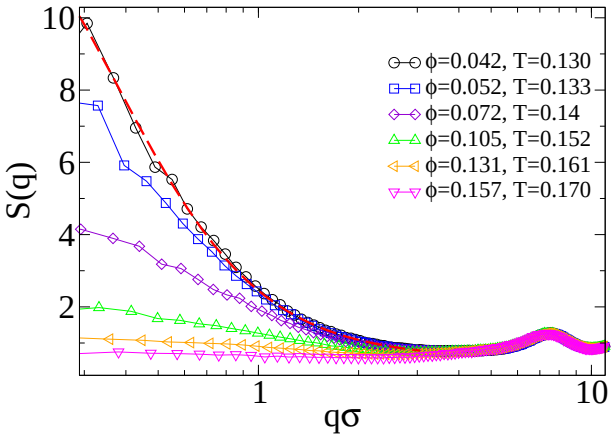

Figure 5. Static structure factors $S(q)$ as a function of wavevector q along the iso-p_b line with $p_b \sim 0.565$. Fitting the low q behavior to a Lorentzian[49] (dashed line shown in Fig. as an example), we extract the thermal correlation length ξ for each state point.

From the static structure factors we obtain an accurate estimate of the thermal correlation length ξ through a fit of the low wavevector region with a Lorentzian function [20], as also shown in 5.

B. Effective potentials along iso-p_b lines for reversible clusters

The effective potentials $V_{eff}(r)$ of two HS colloids immersed in the 3P sol along the chosen iso-p_b lines are shown in Fig. 6. First of all, we observe that the value of the effective potentials at contact ($V_{eff}(r=0)$) scales with with the sol density, as usually found in standard depletion. Interestingly, the range of the potentials is larger than the cosolute particle size σ which sets the lenght scale of V_{eff} in low-density depletion phenomena by non-aggregating co-solutes. However, we notice that, moving along the iso-p_b line, the range of V_{eff} increases by decreasing the cosolute ρ and T (as magnified in the inset of Fig. 6). Thus, although particles organize into the same distribution of clusters, the contributions of these clusters to the effective potentials are different depending on the considered state point. In the following, we try to connect such observation with the behaviour of the cosolute along the iso-p_b line.

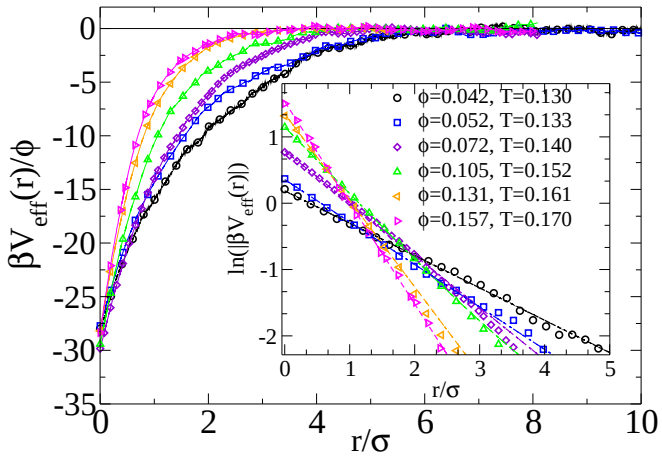

Figure 6. Effective potentials for six state points along the iso-p_b line with $p_b \sim 0.565$. Note that the potentials are scaled by ϕ to show that close to contact they are controlled by the density of depletants as in standard depletion. The inset shows the logarithm of the effective potentials and the corresponding linear fits (dashed lines). The slopes of the fits correspond to the inverse of the range of the potentials.

To do so, we have evaluated the so-called translational order parameter $\tilde{T}$ (not to be confused with temperature), following Ref. [50]. This is defined as,

$$\tilde{T} = \frac{\int_{\sigma\rho^{1/3}}^{r_c} |g(r') - 1| dr'}{r_c - \sigma\rho^{1/3}} \qquad (5)$$

where ρ is the number density, $r' = r\rho^{1/3}$ and r_c is a cutoff value. We have chosen $r_c = 5\sigma$. This observable provides a measure of the thermal correlation length, as it can be seen in Fig. 7 where the behavior of $\tilde{T}$ is reported together with ξ obtained from the static structure factors. Both observables display an identical behavior, showing a clear increase with decreasing ϕ (and T) along the chosen iso-p_b line due to the increasing proximity to the gas-liquid spinodal. To rationalise the

fact that the observed range increases with decreasing ϕ, we have estimated the range $\tilde{r}$ of the effective potentials by performing exponential fits, highlighted in the inset of Fig. 6). Thus, in Fig. 7 we also compare the behavior of $\tilde{r}$ upon moving along the iso-p_b line with the thermal correlation length and find it follows again the same behavior. Thus, the growth in the correlations among the sol particles expressed in the structural correlators is also responsible of the growth of the range of the effective potential. These results allow us to conclude that, in the case of reversible bonds, the effective potential is controlled by thermodynamic, rather than connectivity, properties.

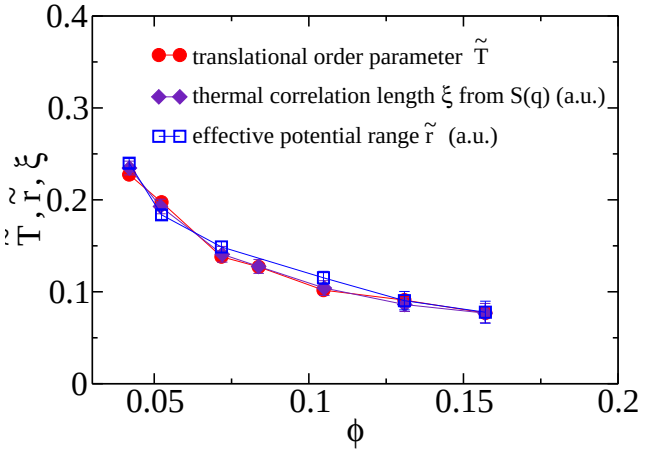
translational order parameter $\tilde{T}$
thermal correlation length ξ from S(q) (a.u.)
effective potential range $\tilde{r}$ (a.u.)
$\tilde{T}, \tilde{r}, \xi$
ϕ

Figure 7. Translational order parameter $\tilde{T}$, thermal correlation length ξ and (scaled) range of reversible effective potential $\tilde{r}$ versus packing fraction of the cosolute along the chosen iso-p_b line. The cutoff value r_c in the integral of Eqn 5 is set to 5. Error bars are estimated by the fits of $S(q)$ at low q for ξ and of V_{eff} for $\tilde{r}$. We note that a different definition of the potential range, e.g. by fitting a third order polynomial to V_{eff} and extracting the value at which the potential is equal to zero gives consistent results.

We recall that, if the cluster bonds have infinite life time, the scenario is significantly different, since in that case it is the connectivity length of the clusters in the sol which controls the range of the effective potentials [34]. Thus, when two colloids are immersed in such sol of clusters they experience an effective potential whose range is independent on the density but depends only on the connectivity properties of the system. This is shown in Fig. 8, where the effective potentials in the case of irreversible clusters are shown in log scale for two state points along the iso-p_b line together with the corresponding potentials for the reversible clusters case. We find that the decay of the two potentials for irreversible clusters are well described by exponential functions having the same decay length as shown in the figure, highlighting that the range is the same along the iso-p_b lines. This is of course different from the behaviour for the reversible cluster case. The inset of Fig. 8 also shows that the range of V_{eff} for irreversible clusters is by far larger than that for reversible ones. This difference between reversible and irreversible clusters already teaches us that for reversible clusters the observed effective potentials cannot be modeled in terms of ideal depletion from a polydisperse sol, despite we have found that $\beta V_{eff}(0)$ scales with the sol density, as predicted by standard depletion approaches.

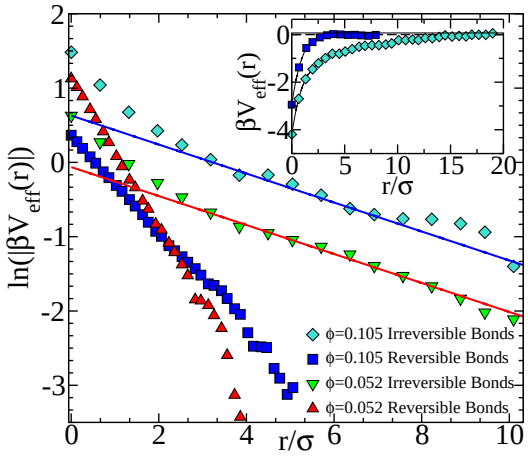

Figure 8. Effective potentials for reversible and irreversible clusters for two different state points along the chosen isop_b line. Straight lines are exponential fits to the tails of the irreversible V_{eff}, having the same decay length for both state points. Inset: comparison of V_{eff} for $\phi = 0.105$ for reversible and irreversible clusters.

C. Effect of the bond lifetime on the effective potentials

So far, we have established that colloids immersed in a sol forming respectively reversible or irreversible clusters experience rather different effective potentials. In the first case, the range of the effective potential is set by the thermal correlation among the particles and seems not to be mediated by clusters, while in the second case clusters act as depletants and indeed the resulting V_{eff} has been successfully interpreted through a depletion model. Thus, one could be tempted to ask whether the lifetime of the clusters plays any role, and if such clusters become sufficiently long-lived, whether they contribute to the effective potentials, for example providing a different V_{eff} bridging the fully reversible (thermal) and irreversible (geometric) case in a continuous way.

To this aim, we have added an infinitesimal barrier to the 3P square-well interaction. First, we have evaluated the properties of the system for several values of the height h of the barrier. While we find that structural and thermodynamic properties, such as $g(r)$ and energy, are

identical upon increasing h, the MC dynamics of the system is largely affected by the introduction of the barrier, in agreement with previous works[35–37]. This is shown in Fig. 9 where the bond correlation function is reported for various values of h. The associated bond relaxation time τ_B is also reported, displaying a clear crossover to an Arrhenius behavior at large enough h.

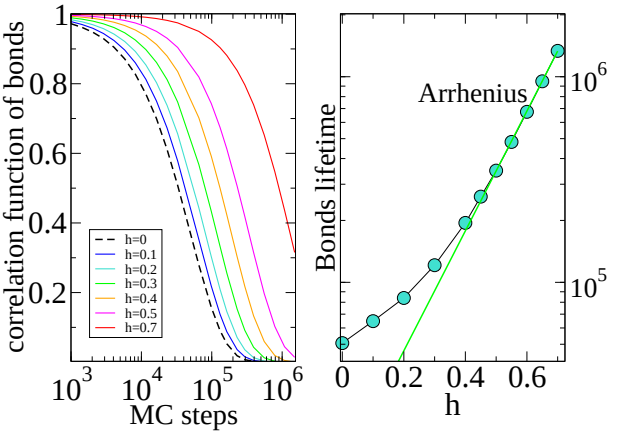

Figure 9. Left panel: bond correlation function for a 3P sol in the presence of an additional barrier with several values of height h. Right panel: the associated bond lifetime τ_B as a function of h, highlighting the onset of Arrhenius behavior at large enough (i.e. $h \gtrsim 0.5$) barrier heights.

We thus repeat the evaluation of the effective potential in the presence of the barrier, for $h = 0.7$, where an increase of the bond lifetime by more than one order of magnitude with respect to the fully reversible case ($h = 0$) is observed. The resulting V_{eff} is reported in Fig. 10 in comparison with the $h = 0$ case. We find that the two potentials are identical, i.e. no effect of the bond lifetime of the clusters is recorded on the effective potentials. Thus, V_{eff} jumps discontinuously from the behaviour for reversible clusters of *any* finite lifetime, which is always controlled by the underlying thermal correlations of the suspending sol, to the behavior for irreversible clusters, that is singular and only happens in the case of infinite bond lifetime.

IV. CONCLUSIONS

In this work we have investigated the effective potentials among colloids in a self-assembling cosolute. In particular, we have studied state points where the cosolute is close to percolation, moving along a path where the bond probability is constant and the cluster size distribution is identical. The resulting effective potentials are found to depend, at short distances, on the density of the cosolute, in agreement with depletion arguments. But at

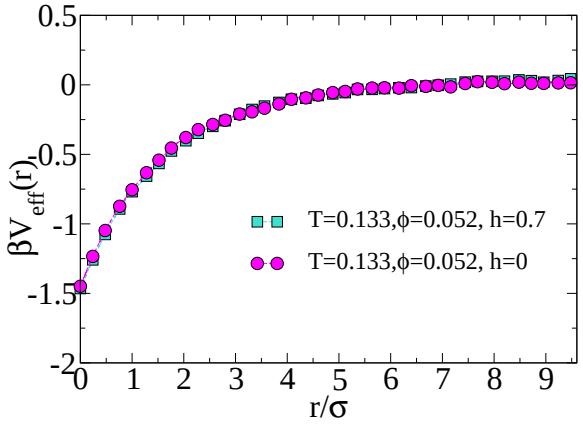

Figure 10. Effective potential for two colloids immersed in a 3P sol at $\phi = 0.052, T = 0.133$ for reversible clusters with ($h = 0.7$) and without ($h = 0$) the addition of an infinitesimal barrier, which modulates the bond (and clusters) lifetime.

long distances they display an increasing range of interaction upon decreasing ϕ and T. The reversible clusters results differ with previous findings for irreversible clusters (despite the same cluster size distribution and average density), which did not show any dependence in the range on the chosen state points. This is because under conditions of irreversible bonds the potentials are slaved to the geometric properties of the clusters, which act as non-interacting highly polydisperse rigid bodies generating a depletion-like potential on the colloids. Our finding show that when clusters can break and reform on timescale shorter than the experimental time scale, the cluster identity is lost and the effective potentials depends only on the thermal correlation length of the sol.

In order to identify whether the case of irreversible bonds represents a singular limit or can be accessed in a continuous way, we have also investigated the effect of bond lifetime, which we appropriately tune by introducing an infinitesimal barrier in the cosolute attractive potential. We find that, even in the case of a large but finite lifetime, the resulting effective potentials experienced by colloids coincide with those obtained for reversible clusters where the bond lifetime is short. Thus, the bond lifetime, whenever finite, does not play any role on V_{eff}, as long as the system can probe all micro states of the sol, e.g. the measurement time of V_{eff} is long enough. Under these conditions, colloids experience the same effective interactions independently of how often cluster break and reform. In this respect, the irreversible case remains a distinct physical situation, and one cannot interpolate continuously from one case to another.

Our work has a direct relevance for experimental situations when aggregation of a second component, being it a solvent or a cosolute, is exploited to induce ad-

hoc effective interactions. Only when the sol is chemical, forming clusters that cannot be broken, a Casimir-like effect induced by cluster confinement is found. For physical sols, a shorter-ranged potential which is dictated solely by thermal properties of particles (and not of clusters) is recovered. Thus, in most physical realizations, the "physical" picture applies, which is not simply interpreted in terms of ideal depletion arguments, except for short colloid-colloid distances.

V. ACKNOWLEDGEMENTS

NG and EZ acknowledge support from MIUR ("Futuro in Ricerca" ANISOFT/RBFR125H0M) and from the European Research Council (ERC Consolidator Grant 681597, MIMIC). FS and EZ acknowledge support from ETN-COLLDENSE (H2020-MCSA-ITN-2014, Grant No. 642774).

[1] Christos N Likos. Effective interactions in soft condensed matter physics. Physics Reports, 348(4):267–439, 2001.

[2] Sho Asakura and Fumio Oosawa. Interaction between particles suspended in solutions of macromolecules. Journal of polymer science, 33(126):183–192, 1958.

[3] A Vrij. Polymers at interfaces and the interactions in colloidal dispersions. Pure and Applied Chemistry, 48(4):471–483, 1976.

[4] WCK Poon, JS Selfe, MB Robertson, SM Ilett, AD Pirie, and PN Pusey. An experimental study of a model colloid-polymer mixture. Journal de Physique II, 3(7):1075–1086, 1993.

[5] Y Mao, ME Cates, and HNW Lekkerkerker. Depletion force in colloidal systems. Physica A: Statistical Mechanics and its Applications, 222(1):10–24, 1995.

[6] Marjolein Dijkstra, René van Roij, and Robert Evans. Phase diagram of highly asymmetric binary hard-sphere mixtures. Physical Review E, 59(5):5744, 1999.

[7] Marjolein Dijkstra, Joseph M Brader, and Robert Evans. Phase behaviour and structure of model colloid-polymer mixtures. Journal of Physics: Condensed Matter, 11(50):10079, 1999.

[8] Stefano Buzzaccaro, Roberto Rusconi, and Roberto Piazza. Sticky hard spherse: equation of state, phase diagram, and mestastable gels. Physical review letters, 99(9):098301, 2007.

[9] Peter J. Lu, Emanuela Zaccarelli, Fabio Ciulla, Andrew Schofield, Francesco Sciortino, and David A. Weitz. Gelation of particles with short-range attraction. Nature, (453):499, 2008.

[10] Henk NW Lekkerkerker and Remco Tuinier. Colloids and the depletion interaction, volume 833. Springer, 2011.

[11] Nathan A Mahynski, Athanassios Z Panagiotopoulos, Dong Meng, and Sanat K Kumar. Stabilizing colloidal crystals by leveraging void distributions. Nature communications, 5, 2014.

[12] Douglas J Ashton, Robert L Jack, and Nigel B Wilding. Porous liquid phases for indented colloids with depletion interactions. Physical review letters, 114(23):237801, 2015.

[13] Lorenzo Rovigatti, Nicoletta Gnan, Alberto Parola, and Emanuela Zaccarelli. How soft repulsion enhances the depletion mechanism. Soft Matter, 11(4):692–700, 2015.

[14] ME Fisher and PG de Gennes. Cr acad. sci. paris ser. B, 287:207, 1978.

[15] Christopher Hertlein, L Helden, A Gambassi, S Dietrich, and C Bechinger. Direct measurement of critical casimir forces. Nature, 451(7175):172–175, 2008.

[16] Daniel Bonn, Jakub Otwinowski, Stefano Sacanna, Hua Guo, Gerard Wegdam, and Peter Schall. Direct observation of colloidal aggregation by critical casimir forces. Physical review letters, 103(15):156101, 2009.

[17] John R Edison, Nikos Tasios, Simone Belli, Robert Evans, René van Roij, and Marjolein Dijkstra. Critical casimir forces and colloidal phase transitions in a near-critical solvent: A simple model reveals a rich phase diagram. Physical review letters, 114(3):038301, 2015.

[18] Hendrik Hobrecht and Alfred Hucht. Many-body critical casimir interactions in colloidal suspensions. Physical Review E, (92):042315, 2015.

[19] Stefano Buzzaccaro, Jader Colombo, Alberto Parola, and Roberto Piazza. Critical depletion. Physical review letters, 105(19):198301, 2010.

[20] Nicoletta Gnan, Emanuela Zaccarelli, Piero Tartaglia, and Francesco Sciortino. How properties of interacting depletant particles control aggregation of hard-sphere colloids. Soft Matter, 8(6):1991–1996, 2012.

[21] Nicoletta Gnan, Emanuela Zaccarelli, and Francesco Sciortino. Tuning effective interactions close to the critical point in colloidal suspensions. The Journal of chemical physics, 137(8):084903, 2012.

[22] A Gambassi, A Maciołek, C Hertlein, U Nellen, L Helden, C Bechinger, and S Dietrich. Critical casimir effect in classical binary liquid mixtures. Physical Review E, 80(6):061143, 2009.

[23] Sathyanarayana Paladugu, Agnese Callegari, Yazgan Tuna, Lukas Barth, Siegfried Dietrich, Andrea Gambassi, and Giovanni Volpe. Nonadditivity of critical casimir forces. Nature communications, 7, 2016.

[24] O Zvyagolskaya, Andrew J Archer, and C Bechinger. Criticality and phase separation in a two-dimensional binary colloidal fluid induced by the solvent critical behavior. EPL (Europhysics Letters), 96(2):28005, 2011.

[25] Stefano Buzzaccaro, Roberto Piazza, Jader Colombo, and Alberto Parola. When depletion goes critical. Journal of Physics: Condensed Matter, (23):194114, 2011.

[26] Suzanne Faber, Zhibing Hu, Gerard H Wegdam, Peter Schall, et al. Controlling colloidal phase transitions with critical casimir forces. Nature communications, 4:1584, 2013.

[27] Minh Triet Dang, Ana Vila Verde, Peter G Bolhuis, Peter Schall, et al. Temperature-sensitive colloidal phase behavior induced by critical casimir forces. The Journal

of chemical physics, 139(9):094903, 2013.
[28] TR Kirkpatrick, JM Ortiz de Zárate, and JV Sengers. Nonequilibrium casimir-like forces in liquid mixtures. Physical review letters, 115(3):035901, 2015.
[29] D Ray, C Reichhardt, and CJ Olson Reichhardt. Casimir effect in active matter systems. Physical Review E, 90(1):013019, 2014.
[30] Ran Ni, Martien A Cohen Stuart, and Peter G Bolhuis. Tunable long range forces mediated by self-propelled colloidal hard spheres. Physical review letters, 114(1):018302, 2015.
[31] C Cattuto, R Brito, U Marini Bettolo Marconi, F Nori, and R Soto. Fluctuation-induced casimir forces in granular fluids. Physical review letters, 96(17):178001, 2006.
[32] A. Aminov, Y. Kafri, and M. Kardar. Fluctuation-induced forces in nonequilibrium diffusive dynamics. Physical review letters, (114):230602, 2015.
[33] Akira Furukawa, Andrea Gambassi, Siegfried Dietrich, and Hajime Tanaka. Nonequilibrium critical casimir effect in binary fluids. Physical review letters, 111(5):055701, 2013.
[34] Nicoletta Gnan, Emanuela Zaccarelli, and Francesco Sciortino. Casimir-like forces at the percolation transition. Nature communications, 5, 2014.
[35] Emanuela Zaccarelli, Giuseppe Foffi, Francesco Sciortino, and Piero Tartaglia. Activated bond-breaking processes preempt the observation of a sharp glass-glass transition in dense short-ranged attractive colloids. Physical review letters, 91(10):108301, 2003.
[36] I Saika-Voivod, E Zaccarelli, Francesco Sciortino, SV Buldyrev, and P Tartaglia. Effect of bond lifetime on the dynamics of a short-range attractive colloidal system. Physical Review E, 70(4):041401, 2004.
[37] Anshul DS Parmar and Srikanth Sastry. Kinetic and thermodynamic fragilities of square well fluids with tunable barriers to bond breaking. The Journal of Physical Chemistry B, 119(34):11243–11252, 2015.
[38] Norbert Kern and Daan Frenkel. Fluid–fluid coexistence in colloidal systems with short-ranged strongly directional attraction. The Journal of chemical physics, 118(21):9882–9889, 2003.
[39] To account for the presence of the barrier we modify the Metropolis acceptance rule by introducing a penalty in the energy whenever bonds among particles are formed or broken. In particular, given the energy of the new configuration that needs to be accepted or refused, we account for broken bonds $N_b r$ by adding a positive contribution $V_b = N_b r \cdot (\varepsilon + h)$. Analogously, if new bonds N_f are formed, the energy is modified by the quantity $V_f = N_f \cdot h$. Note that the modified energies are only used in the Boltzmann factor entering in the Metropolis rule and do not correspond to real energies of the system.
[40] Emanuela Bianchi, Julio Largo, Piero Tartaglia, Emanuela Zaccarelli, and Francesco Sciortino. Phase diagram of patchy colloids: towards empty liquids. Physical review letters, 97(16):168301, 2006.
[41] MS Wertheim. Fluids with highly directional attractive forces. i. statistical thermodynamics. Journal of statistical physics, 35(1-2):19–34, 1984.
[42] MS Wertheim. Fluids with highly directional attractive forces. ii. thermodynamic perturbation theory and integral equations. Journal of statistical physics, 35(1-2):35–47, 1984.
[43] MS Wertheim. Fluids with highly directional attractive forces. iii. multiple attraction sites. Journal of statistical physics, 42(3-4):459–476, 1986.
[44] MS Wertheim. Fluids with highly directional attractive forces. iv. equilibrium polymerization. Journal of statistical physics, 42(3-4):477–492, 1986.
[45] Nicoletta Gnan, Daniel De Las Heras, José Maria Tavares, Margarida M Telo Da Gama, and Francesco Sciortino. Properties of patchy colloidal particles close to a surface: A monte carlo and density functional study. The Journal of chemical physics, 137(8):084704, 2012.
[46] Emanuela Bianchi, Piero Tartaglia, Emilia La Nave, and Francesco Sciortino. Fully solvable equilibrium self-assembly process: Fine-tuning the clusters size and the connectivity in patchy particle systems. J. Phys. Chem. B, (111):11765, 2007.
[47] Emanuela Bianchi. Equilibrium Behavior of Patchy Particles: Thermoreversible Gelation, Phase Separation and Self-Assembly. PhD thesis, PhD thesis, 2008.
[48] Francesco Sciortino and Emanuela Zaccarelli. Reversible gels of patchy particles. Current Opinion in Solid State and Materials Science, 15(6):246–253, 2011.
[49] Jean-Pierre Hansen and Ian R McDonald. Theory of simple liquids. Elsevier, 1990.
[50] Thomas M Truskett, Salvatore Torquato, and Pablo G Debenedetti. Towards a quantification of disorder in materials: distinguishing equilibrium and glassy sphere packings. Physical Review E, 62(1):993, 2000.